AIAA AVIATION Forum
5-9 June 2017, Denver, Colorado
23rd AIAA/CEAS Aeroacoustics Conference

AIAA 2017-3015

Passive Control of the Vortex Shedding Noise of a Cylinder at Low Reynolds Numbers Using Flexible Flaps

Thomas F. Geyer[*]
Brandenburg University of Technology Cottbus - Senftenberg, 03046 Cottbus, Germany

Laura Kamps[†]
Technical University Bergakademie Freiberg, 09599 Freiberg, Germany

Ennes Sarradj[‡]
Technische Universität Berlin, 10587 Berlin, Germany

Christoph Brücker[§]
City University London, London EC1V 0HB, United Kingdom

A recent experimental study on the vortex shedding noise of a cylinder equipped with thin, flexible flaps showed that the presence of the flaps leads to a sudden shift of the aeolian tones when above a certain Reynolds number, which resulted in a jump in the corresponding Reynolds-Strouhal number diagram. In the present work, this effect is further investigated by performing acoustic measurements on modified versions of the original flap cylinder, where, subsequently, flaps were cut off to study their individual contribution to the vortex shedding. In addition to the acoustic measurements, the movement of the flaps was captured using a high-speed camera. The eigenmodes of the flaps were calculated numerically. The results confirm that the jump of the Strouhal number is caused by a lock-in of the vortex shedding cycle with the oscillation of the outer flaps at the next higher eigenfrequency. Reducing the number of flaps does not affect the jump, but a shortening of the flaps (and hence a modification of the flap eigenmodes) lead to the fact that the Strouhal number jumped to a lower value than before.

I. Introduction

Vortex shedding from cylinders is a classical problem in aerodynamics and an important source of noise. The understanding of passive means to control the vortex shedding, such as surface protrusions, shrouds and nearwake stabilizers [1], splitter plates [2, 3], O-rings [4], grooves [5], tripping wire [6], riblets [7] or porous material [8], is therefore of great interest for many potential applications.

In a water tunnel study by Kunze and Brücker [9] it has been shown that the presence of flexible flaps at the aft part of a circular cylinder strongly affects the vortex shedding behaviour. This lead to the fact that at a certain specific Reynolds number (based on cylinder diameter) the Strouhal number associated with vortex shedding quite suddenly increased, resulting in a jump in the corresponding Reynolds-Strouhal number diagram. The reason for this effect was found to be a lock-in effect between the vortex shedding and the oscillation of the flexible flaps, which compose a resonator (caused by the visco-elastic coupling of the flap system). Additionally, Particle Image Velocimetry (PIV) measurements showed that, due to the presence of the flaps, the vortices were not shed in a zig-zag like arrangement as in the classical von Kármán

[*]Research Assistant, Chair of Technical Acoustics, Brandenburg University of Technology Cottbus - Senftenberg, Germany.
[†]Research Assistant, Institute for Mechanics and Fluid Dynamics, Technical University Bergakademie Freiberg, Germany.
[‡]Professor, Institute of Fluid Mechanics and Engineering Acoustics, Technische Universität Berlin, Germany.
[§]Professor, BAE SYSTEMS Sir Richard Olver Chair in Aeronautical Engineering, City University London, United Kingdom.

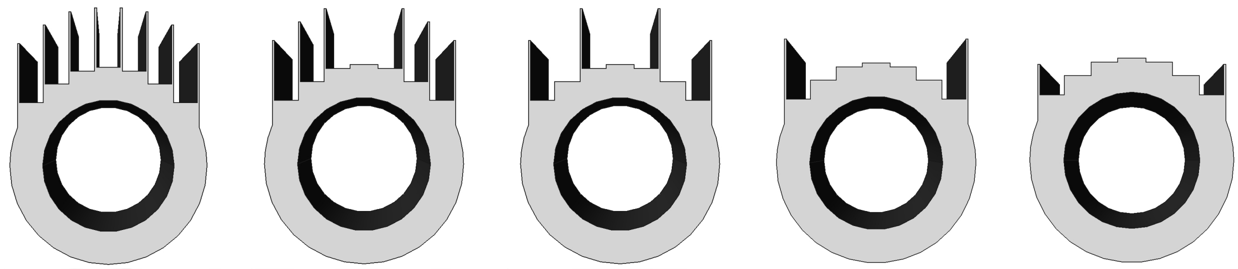

(a) 8 flaps (b) 6 flaps (c) 4 flaps (d) 2 flaps (e) 2 flaps, shortened

Figure 1. CAD models of the different flap ring versions used for the study

vortex street, but rather in-line in a row with the cylinder wake axis. A subsequent investigation [10], which was performed in an aeroacoustic wind tunnel, revealed that the change in vortex shedding also effected the emission of tonal noise, as the aeolian tones generated by a cylinder modified with eight flexible flaps were shifted to higher frequencies when above a certain Reynolds number. The resulting jump of the corresponding Strouhal number was accompanied by a shift of the peak of the turbulent velocity fluctuations measured inside the shear layer. It was concluded that the jump of the Strouhal number is caused by a lock-in between the vortex shedding peak and the resonances of the flap structures. Additionally, it was concluded that the outer flaps play a more important role than the inner flaps since they interact directly with the shear layer.

The present study is a continuation of the work presented in [10]. Thereby, the focus is to further examine the fluid-structure-interaction and the assumed cause of the Strouhal number jump. To this end, a set of measurements was performed on the original flap cylinder with eight flaps (as used in [10]) as well as on modified versions where, subsequently, flaps were cut off in order to determine their individual contribution to the observed vortex shedding behavior.

II. Materials and Methods

II.A. Cylinder Models

The flap cylinders consist of a core cylinder with a length of 0.28 m and a diameter of 20 mm, on which 22 flap rings made of the silicone rubber Elastosil RT 601 were threaded. The flap rings were cast using a casting mold consisting of metal plates with small gaps that will form the flaps. The original flap rings, as used in [10], contained eight flaps with a thickness of 0.3 mm. In the present study, measurements were also performed on modified flap rings, where a number of flaps was cut off from the original flap rings, resulting in cylinders with six, four and two flaps instead of eight. Figure 1 shows CAD models of the different flap rings used for this study. In most cases, the flaps had the original length of 9 mm (Figure 1(a) through 1(d)). In the final experiments, the two remaining outer flaps were shortened to a length of 4.5 mm (Figure 1(e)). Additionally, as in [10], a plain cylinder with and without tripping tape was used as a reference in the experiments. The tripping tape had a height of 0.2 mm and a width of 1 mm and was applied at an angle of $\pm 50°$ to the flow over the whole span of the cylinder. All cylinder models had an outer diameter of 30 mm, resulting in an aspect ratio of 9.3. A photograph of the cylinder with six flaps is shown in Figure 2.

II.B. Modal Analysis

In order to enable a better understanding of the observed lock-in effect, the eigenmodes of the flaprings shown in Figure 1 were obtained numerically for frequencies up to 250 Hz using Ansys (Academic Version R15.0). Thereby, the flaprings were modelled as elastic, isotropic materials with a Young's modulus of 1.2 MPa, a density of 1080 kg/m^3 and a Poisson ratio of 0.495. The meshes for the FEM calculation consisted of tetrahedral elements with a maximum side length of 1 mm (see Figure 3 as an example). As a boundary condition it was defined that the inner surface of the flap ring (where the flap ring is in contact with the rigid core cylinder) will not be displaced.

It can be expected that the dimensions of the physical models of the flap rings may differ slightly from the CAD models due to the manufacturing process. This is especially true for the thickness of the flaps. To take a certain deviation of the nominal thickness of the flaps of 0.3 mm into account, eigenmodes and

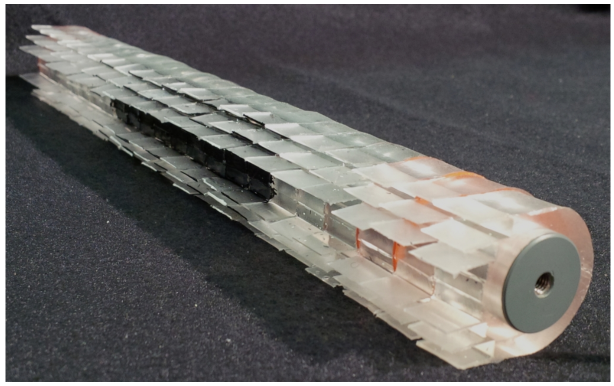

Figure 2. Photograph of the cylinder with six flaps (the flap rings at mid span are painted black to give a better contrast in the flap motion measurements)

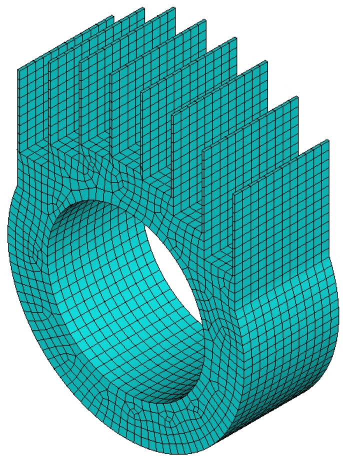

Figure 3. Mesh used for the modal analysis of the original cylinder with eight flaps

eigenfrequencies were additionally obtained for the case that the overall thickness of the flaps was increased by 5 % and 10 % to values of 0.315 mm and 0.33 mm as well as for the cases of a 5 % and 10 % decreased thickness of 0.285 mm and 0.27 mm. Of course, this rather simple procedure does not account for local deviations of the thickness of a single flap.

II.C. Wind Tunnel

The experimental part of the study included acoustic measurements and measurements of the flap motion in the small aeroacoustic wind tunnel at Brandenburg University of Technology Cottbus – Senftenberg [11]. The test section used for the experiments has a rectangular cross-section of 0.28 m height $\times$ 0.23 m width. The top and bottom of this test section are made from acrylic glass, while the two side windows are covered with tensioned Kevlar, thus providing a two-dimensional flow, while at the same time enabling the use of acoustic measurement technique positioned outside of the flow. Surrounding the test section is a cabin with absorbing side walls that lead to a nearly anechoic environment for frequencies above approximately 100 Hz.

Measurements were conducted at 13 subsonic flow speeds between 7 m/s and 17 m/s, leading to Reynolds numbers (based on cylinder diameter) ranging from 14,600 to 34,000. In this range of flow speeds, the vortex shedding noise of the cylinders will be at frequencies below 200 Hz. The blockage due to the cylinders was corrected using the simple approximative blockage correction method proposed by Barlow et al. [12]. In order to obtain a better statistical significance, each measurement was performed twice in individual runs.

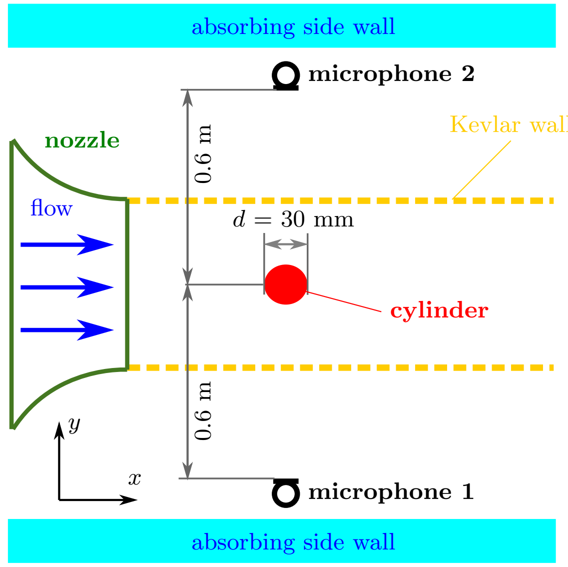

Figure 4. Schematic (top view) of the setup used for the acoustic measurements (not to scale)

II.D. Acoustic Measurements

The acoustic measurements were performed using two single 1/4th inch free-field microphones positioned in a distance of 0.6 m on each side of the cylinder models. In the vertical direction, the microphones were pointed approximately at the mid-span location of the cylinders. Figure 4 shows a schematic of the acoustic measurement setup.

The data were recorded with a sampling frequency of 51.2 kHz over a time period of 90 s, using a 24 Bit National Instruments digital dynamic signal acquisition module (NI-USB 4431). Following the approach used in [10], the time signals from both microphones were added with a phase difference of 180°, assuming a theoretical dipole behaviour of the cylinder generated noise. The data were then transformed in the frequency domain according to Welsh's method [13] using a Fast Fourier Transformation (FFT) with a Hanning window on 50 % overlapping blocks of 131,072 samples each and converted to sound pressure levels *re* 20 μPa. The resulting frequency step size is only 0.39 Hz. Finally, 6 dB were subtracted to correct for the increased amplitude due to the summation of both time signals.

II.E. Flap Motion Measurements

The movement of the flexible flaps of a flap ring, positioned at mid-span, was measured using a high speed camera (Phantom V12.1-8 G-M, Vision Research) with a 35 mm Nikon lens, which was positioned below the test section (see Figure 5). The frame rate was set to 500 Hz with a total measurement duration of approximately 14 s. The exposure time per frame was 500 μs. Using the procedure described in [10], the time-series of the movement of the centroid point of each single flap of a chosen flap ring was derived from the camera recordings. These results were then converted to corresponding power spectral densities of the flap movement using a Burg algorithm [14].

Due to the fact that neighboring flaps are likely to collide at high flow speeds, the flap motion measurements were only performed up to Reynolds numbers of 26,000 to 28,500. For the case of the cylinder with six flaps, however, those measurements could only be conducted up to a Reynolds number of 20,900.

III. Results

III.A. Modal Analysis

The numerical modal analysis revealed that, for all cases where the flaps were not shortened (Figure 1(a) through 1(d)), the eigenmodes and eigenfrequencies in the examined range up to 250 Hz are identical. For example, the first eigenfrequency at 22 Hz, corresponding to the first bending mode of the flap, occurs eight

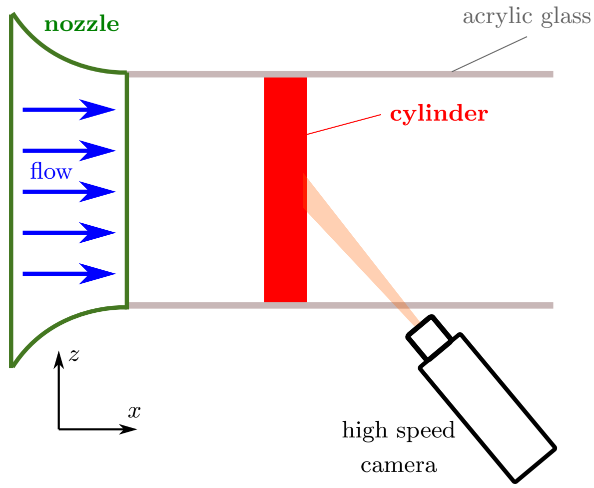

Figure 5. Schematic (side view) of the setup used for the flap motion measurements (not to scale)

Table 1. Numerically obtained eigenfrequencies of the different flap rings shown in Figure 1

flap rings	**eigenfrequencies (Hz)**						
	1st	**2nd**	**3rd**	**4th**	**5th**	**6th**	**7th**
8 flaps	22 (1st bending mode)	39 (1st torsion mode)	97 (2nd torsion mode)	137	156	236	243
6 flaps	22 (1st bending mode)	39 (1st torsion mode)	97 (2nd torsion mode)	137	156	236	243
4 flaps	22 (1st bending mode)	39 (1st torsion mode)	97 (2nd torsion mode)	137	156	236	243
2 flaps	22 (1st bending mode)	39 (1st torsion mode)	97 (2nd torsion mode)	137	156	236	243
2 flaps, shortened	86 (1st bending mode)	107 (1st torsion mode)	171 (2nd torsion mode)	-	-	289	-

times for the original flap ring (Figure 1(a)), six times for the flap ring where the two innermost flaps are cut off (Figure 1(b)), and so on. The second mode (the first torsion mode) can be observed at a frequency of 39 Hz, while the third mode, which appears to be the second torsion mode, is visible at 97 Hz. Another bending mode, but in a direction perpendicular to the first bending mode at 22 Hz, occurs at 137 Hz. Due to the fact that the flaps are firmly attached to the cylinder body, the resulting shape of that particular mode resembles a cambered surface. Further eigenfrequencies of 156 Hz, 236 Hz and 243 Hz were found, the corresponding modes, however, take more complex shapes. Figure 6 shows the shapes of the first seven eigenmodes of one flap from the original flapring with eight flaps.

For the case where the remaining two outer flaps were shortened (see Figure 1(e)), the modal analysis revealed completely different eigenmodes and eigenfrequencies. For example, the frequency of the first bending mode increases to a value of 86 Hz, that of the first torsion mode to 107 Hz and that of the second torsion mode to 171 Hz. Table 1 lists the eigenfrequencies of the different flap rings.

When the thickness of the flaps is increased or decreased by 5 % compared to their nominal thickness of 0.3 mm, the corresponding eigenfrequencies increase/decrease by about 3 to 5 % as well. If the thickness increases/decreases by 10 %, the eigenfrequencies subsequently show an increase/decrease of about 8 to 10 %.

III.B. Results from Acoustic Measurements

The sound pressure level spectra measured for the cylinders from Figure 1 as well as for the tripped and untripped reference cylinder are shown in Figure 7 as a function of Strouhal number based on the outer diameter. Basically, the above discussed effect that the vortex shedding peak obtained for the flap cylinders

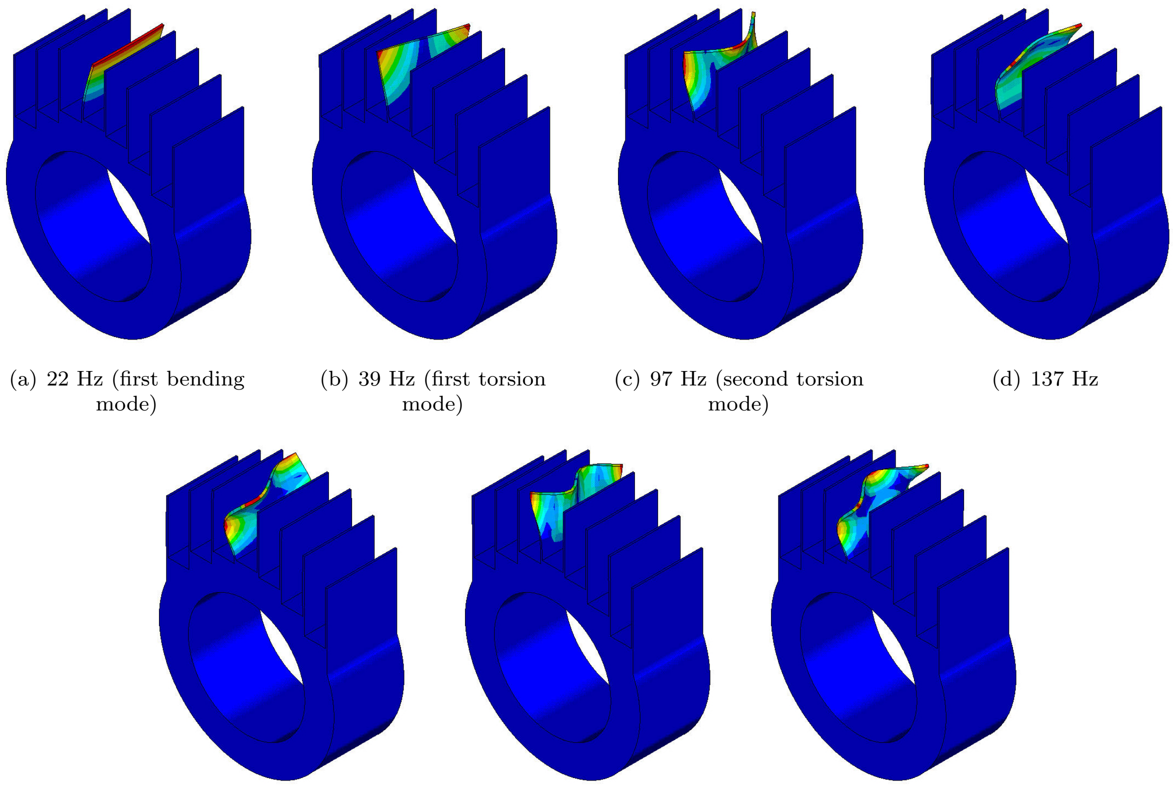

(a) 22 Hz (first bending mode)
(b) 39 Hz (first torsion mode)
(c) 97 Hz (second torsion mode)
(d) 137 Hz
(e) 156 Hz
(f) 236 Hz
(g) 243 Hz

Figure 6. First seven eigenmodes of the original flapring with eight flaps

suddenly jumps towards a higher Strouhal number at Reynolds numbers between 23,300 and 26,000 is visible, while the peaks of the two reference cylinders stay at a constant value just above 0.2. Thereby, the spectra obtained for the cases with unshortened flaps all show essentially the same behavior, while the peak obtained for the cylinder with the two shortened flaps (Figure 1(e)) jumps to a noticeably lower Strouhal number. This implies that, in air, the observed jump is not caused by an oscillation of the flap system as a whole (consisting of eight equally-spaced flaps with a fluid volume in between), but essentially by the movement of the outer flaps. This means that, in the present case, the dominating mechanism is a manipulation of the boundary layer around the cylinder and, most likely, the locations of separation, by the outer flaps. In contrast, in the water tunnel experiments in [9], the lock-in was found to occur between the vortex shedding and a traveling wave running through the bundle of flexible flaps in a direction perpendicular to the flow and the cylinder axis. This difference is presumably caused by the different properties of the two fluids, since in water the coupling between the single flaps is much stronger than in air.

To further illustrate the differences between the cases with the long flaps and the shortened flaps, Figure 8 shows the peak Strouhal number as a function of the Reynolds number based on cylinder diameter. Thereby, this peak Strouhal number represents the arithmetic mean of the peak Strouhal numbers from both measurements. While the resulting Strouhal number for the original cylinder with eight flaps suddenly jumps from values around 0.25 at $Re \leq 23{,}300$ to a value of about 0.3 at $Re = 26{,}000$, the Strouhal number for the cylinder with shortened flaps changes from about 0.24 at $Re = 23{,}300$ to approximately 0.26 at $Re = 26{,}000$. For the reference cylinders, the Strouhal number takes values between 0.22 at the lowest Reynolds number and 0.21 at the highest Reynolds number, which is in good agreement with the theoretical value of 0.21 [15] known for this flow regime (the subcritical range, characterized by a laminar near-wake with vortex street instability). The tripping tape only has a small effect on the Strouhal number, as it seems to lead to a slight increase of the effective cylinder diameter.

Since it was shown in [10] that the aeolian tones generated by the flap cylinder are linked to the movement of the flaps, the following section will provide results from the flap motion measurements.

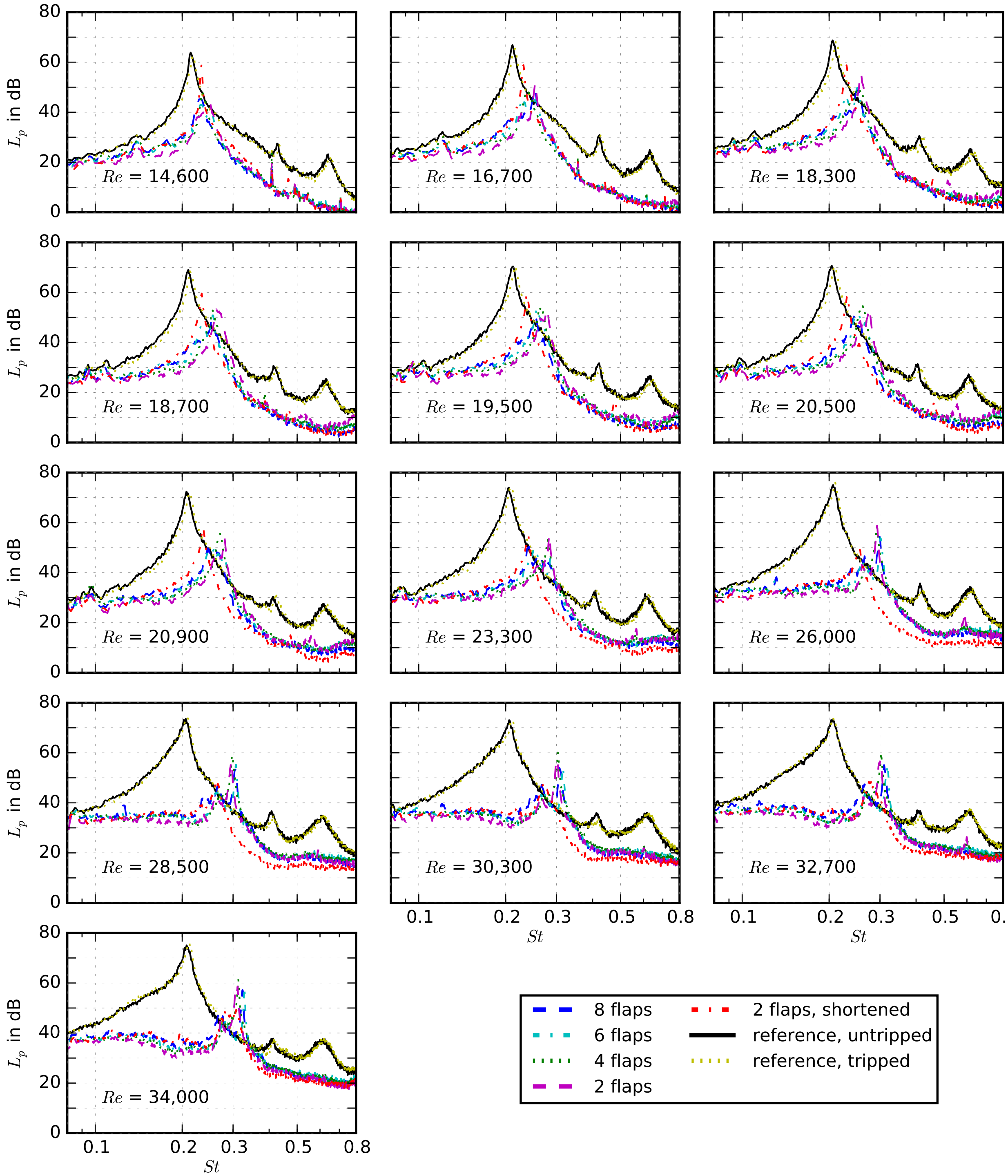

Figure 7. Measured sound pressure level spectra (*re* $2{\cdot}10^{-5}$ Pa) around the vortex shedding peak

III.C. Results from Flap Motion Measurements

Figure 9 shows spectra obtained from the flap motion measurements performed with the high-speed camera. As an example, spectra are shown for one outer flap of all cylinders examined: the original flap cylinder with eight flaps (Figure 1(a)), the cylinder with six flaps (Figure 1(b)), the cylinder with four flaps (Figure 1(c)), the cylinder with two flaps (Figure 1(d)) and that with the two shortened flaps (Figure 1(e)). Each figure additionally contains the theoretical eigenfrequencies derived from the modal analysis as given in Table 1.

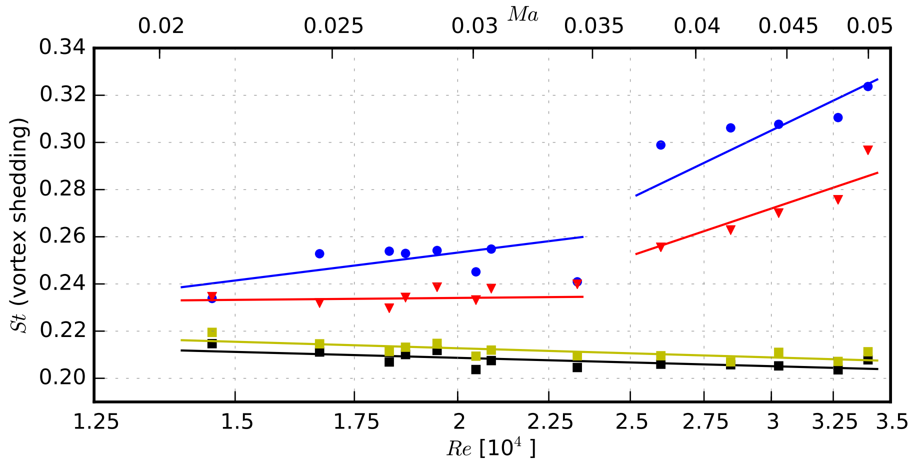

Figure 8. Dependence of the peak Strouhal number St obtained from the acoustic measurements on the Reynolds number Re based on cylinder diameter, the line represents a linear approximation of the measured data (■ baseline cylinder, ■ baseline, tripped, ● 8 flaps, ▼ 2 flaps, shortened)

Also included are the resulting eigenfrequency ranges derived numerically when a deviation of the flap thickness of ±10 % is assumed.

It is visible that the spectra obtained for the original flap cylinder (upper left in Figure 9) are basically similar to those obtained for the cylinder with six flaps (upper right in Figure 9), four flaps (center left) and that with two flaps (center right). The first peak seems to be linked to the first bending mode at 22 Hz or the first torsion mode at 39 Hz. The second peak, at frequencies above 50 Hz, can be associated with vortex shedding, as its frequency increases with increasing Reynolds number. The third peak is at a constant frequency of approximately 170 Hz. When the differences between a CAD model and the actual flap cylinders are taken into account, this third peak may be related to the eigenmode observed at 156 Hz. Interestingly, at very high Reynolds numbers the shape of the flap motion spectra differs from that obtained at lower Reynolds numbers for some of the flap cylinders. Most notably, this includes a shift of the first and strongest spectral peak towards higher frequencies, but in some cases also a generally increased amplitude of the flap movement. For example, for the original eight-flap cylinder, the first spectral peak shifts toward the frequency of the first torsion mode at the highest Reynolds number of 26,000. For the cylinder with only two flaps, the shift of the first peak already occurs at even lower Reynolds numbers, starting approximately at $Re = 18{,}700$.

In the spectra obtained for the cylinder with eight flaps and that with four flaps (upper left and center left in Figure 9), the measurement at the highest Reynolds number of 26,000 belongs to a case where the Strouhal number obtained from the acoustic measurements jumped to a notably higher value of around 0.3. This corresponds to a frequency of about 131 Hz. Around this frequency, the flap motion spectra show a strong peak, which can be assumed to be related to the eigenmode of the flap rings at 137 Hz, as shown in Figure 6(d). As described in Section III.A, this eigenmode is related to a bending motion of the flaps, although in a direction perpendicular to the first bending mode at 22 Hz. The result is a flap that repeatedly cambers and straightens with a frequency of 137 Hz, a process that is very likely to interact with the adjacent flow and the regular vortex shedding. For the cylinder with only the two outer flaps left (center right in Figure 9), the same observations can be made for the measurements at the highest Reynolds numbers of 26,000 and 28,500. Again, the tonal peak that corresponds to the vortex shedding jumps to a frequency of 127 Hz (at $Re = 26{,}000$) and 140 Hz (at $Re = 28{,}500$). Both frequencies are close to the eigenfrequency of 137 Hz and within the ±10 % error limit derived numerically. It can therefore be concluded that the jump in the Re-St-plot is caused by a lock-in of the vortex shedding cycle with an eigenmode of the (outer) flaps.

The spectra obtained for the cylinder with two shortened flaps (lower left in Figure 9) show considerable differences. At low Reynolds numbers, the first discernible peak is the one related to the vortex shedding (at frequencies above 50 Hz). At the two highest Reynolds numbers of 26,000 and 28,500, this vortex shedding peak is already merged with another peak at a fixed frequency of about 95 Hz, which can be assumed to be related to the first bending mode of the short flaps at a frequency of 86 Hz. Thus, in case of the shortened flaps, the sudden shift of the Strouhal number is caused by a lock-in with the first bending mode of the flaps. A second, much smaller local maximum is visible in the flap motion spectra around 140 Hz. This peak

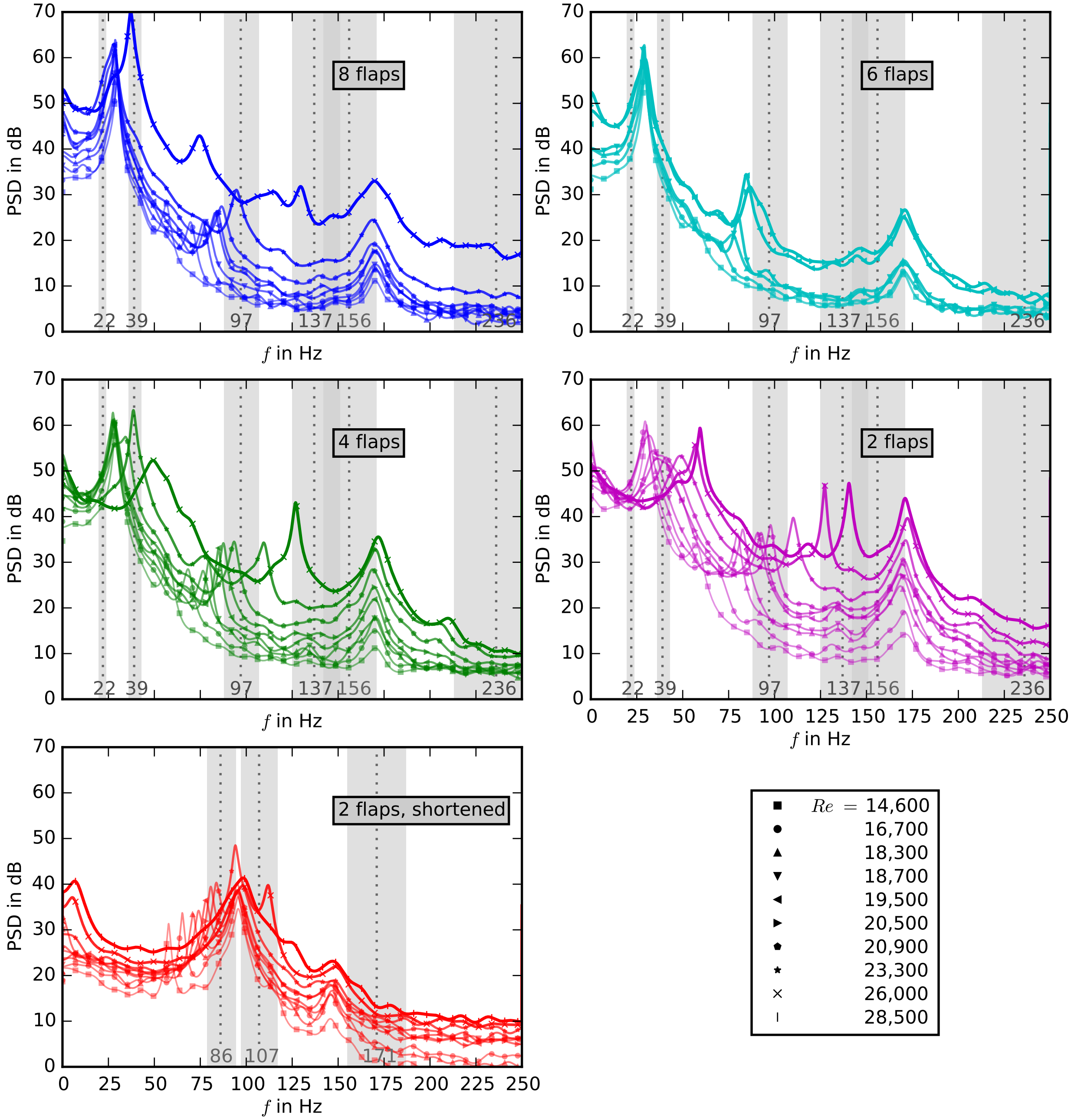

Figure 9. Spectra obtained from the flap motion measurements (vertical lines represent eigenfrequencies obtained numerically, gray bands correspond to deviations in eigenfrequency if a ± 10 % variation of the flap thickness is assumed)

does not seem to be related to any eigenfrequency of the flap ring, as the modal analysis predicted the next eigenmode at a frequency of 170 Hz. The cause of this small peak is currently not clear.

Overall, the present analysis of the flap motion reveals that the observed jump of the Strouhal number related with vortex shedding is caused by a lock-in with an eigenmode of the flaps. In case of the unshortened flaps, this eigenmode belongs to a bending motion of the flaps, but in a direction perpendicular to the first bending mode. For the case with the two shortened flaps, the lock-in happens with the frequency of the first bending mode. It appears, however, that the lock-in always happens with the next "available" mode, and hence the mode with an eigenfrequency just above the natural vortex shedding frequency. It is not fully clear whether the exact shape of this mode is important, as in the present case the corresponding modes were two different bending modes. Basically, this behavior indicates that such effects may also occur at even higher frequencies, when the vortex shedding cycle locks-in with the next higher eigenfrequency. It was not possible to test this hypothesis with the present setup, since with further increasing flow speed neighboring flaps started to collide, rendering the analysis of the flap motion impossible.

IV. Summary

In a recent wind tunnel study by Kamps et al. [10] on the vortex shedding noise generated by a cylinder equipped with eight flexible flaps it was found that the flaps alter the frequency of the vortex shedding. This lead to a sudden jump in the corresponding plot of Strouhal number versus Reynolds number. This jump is visible in the acoustic power spectral density, in the spectra of the turbulent velocity fluctuations inside the shear layer and in the spectra corresponding to the movement of the flaps. It was concluded that the jump is most likely the consequence of a lock-in effect between the natural vortex shedding cycle and the resonance frequency of the system of eight flaps, which forms a coupled oscillator.

The aim of the present study is to further investigate the effect of the flexible flaps on the vortex shedding and the possible cause of the Strouhal number jump. To this end, the original cylinder with eight flaps was modified by subsequently cutting off flaps, until only the two outermost flaps remained. This was done in oder to verify whether all flaps contribute to the Strouhal number jump or if only the outer flaps are necessary. Finally, the remaining outer flaps were additionally shortened in order to investigate the effect of the flap size on the Strouhal number. For each resulting cylinder model, acoustic measurements were performed in an aeroacoustic wind tunnel at low Reynolds numbers, using two microphones on opposite sides of the wind tunnel test section. A high speed camera was used to capture the motion of the flaps of one flap ring approximately at mid span. In addition to the wind tunnel experiments, a modal analysis of the different configurations was performed numerically.

The measurement results revealed that the spectra of the cylinders with flaps of equal length show essentially the same behavior, meaning the Strouhal number jumps to the same value within the same Reynolds number range between 23,300 and 26,000. Thus, the observed lock-in effect does not seem to be caused by an oscillation of a whole system of flaps, but rather by the movement of the two outer flaps, thus affecting the separation of the shear layer.

Additionally, the analysis of the flap motion spectra and a subsequent comparison with the eigenmodes of the single flaps showed that the observed Strouhal number jump is caused by a lock-in of the natural vortex shedding cycle with the next higher eigenfrequency.

Acknowledgements

This work was partly funded within the framework of PEL-SKIN project EU-FP7, GA no. 334954. Funding of the position of Professor Christoph Brücker as the BAE SYSTEMS Sir Richard Olver Chair in Aeronautical Engineering is gratefully acknowledged herein.

References

[1] Zdravkovich, M. M., Review and classification of various aerodynamic and hydrodynamic means for suppressing vortex shedding. Journal of Wind Engineering and Industrial Aerodynamics, 7 (2), 145–189, 1981

[2] Kiyoung, K., Choi, H., Control of laminar vortex shedding behind a circular cylinder using splitter plates, Physics of Fluids 8 (2), 479–486, 1996

[3] Roshko, A., On the wake and drag of bluff bodies, Journal of the Aeronautical Sciences, 2012

[4] Lim, H. C., Lee, S. J., Flow control of a circular cylinder with O-rings. Fluid Dynamics Research, 35 (2), 107–122, 2004

[5] Ko, N. W. M.,Leung, Y. C., Chen, J. J. J., Flow past V-groove circular cylinders. AIAA Journal, 25 (6) 806–811, 1987

[6] Igarashi, T., Effect of tripping wires on the flow around a circular cylinder normal to an airstream. Bulletin of JSME, 29 (255), 2917–2924, 1986

[7] Lee, S. J.,Lim, H. C., Han, M., Lee, S. S., Flow control of circular cylinder with a V-grooved micro-riblet film, Fluid dynamics research, 37 (4), 246–266, 2005

[8] Geyer, T. F., Sarradj, E., Circular Cylinders with Soft Porous Cover for Flow Noise Reduction. Experiments in Fluids, 57(3), 1–16, 2016

[9] Kunze, S., Brücker, C., Control of Vortex Shedding on a Circular Cylinder Using Self-Adaptive Hairy-Flaps. Comptes Rendus Mécanique 340 (1), 41–56, 2012

[10] Kamps, L., Geyer, T. F., Sarradj, E., Brücker, C., Vortex shedding noise of a cylinder with hairy flaps. Journal of Sound and Vibration 388, 69–84, 2017

[11] Sarradj, E., Fritzsche, C., Geyer, T. F., Giesler, J., Acoustic and aerodynamic design and characterization of a small-scale aeroacoustic wind tunnel, Appl Acoust, 70, 1073-1080, 2009

[12]Barlow, J. B., Rae, W. H., Pope, A., Low-speed wind tunnel testing. Third edition, John Wiley & Sons, 1999

[13]Welsh, P. D., The use of fast Fourier transform for the estimation of power spectra: a method based on time averaging over short, modified periodograms. IEEE Trans. Audio and Electroacoustics, 15(2), 70-73, 1967

[14]Stoica, P., Moses, R., Introduction to Spectral Analysis. Prentice-Hall, Upper Saddle River, NJ, 1997

[15]Schlichting, H., Gersten, K., Boundary-layer theory. Springer Verlag Berlin Heidelberg, 9th edition, 1997